*J. Environ. Nanotechnol.*
*Volume 5, No.2(2016) pp. 48-64*
*ISSN (Print): 2279-0748*
*ISSN (Online): 2319-5541*
*doi:10.13074/jent.2016.06.162195*

# Influence of Hole and Electron Transport Materials on Perovskite Sensitized Solar Cells-A Review

**L. Sampath Kumar[1], D.P. Bhatt[2], S. Karthikeyan[3*]**

[1]*Department of Physics, EBET Group of Institutions, Kangayam, Tiruppur, TN, India.*
[2]*Intellectual Property Rights Management Group, CSIR, National Physical Laboratory, New Delhi, India.*
[*3]*Department of Chemistry, Chikkanna Government Arts College, Tiruppur, TN, India.*

*Received: 26.04.2016 Accepted: 19.06.2016*

***Abstract***

*Organic/Inorganic lead halide perovskite solar cells (PrSCs) have received considerable attention in recent years as the promising materials capable of developing high performance photovoltaic devices due to their high light absorption coefficient, tunable band gap, high carrier mobility, long carrier diffusion length, low temperature processing and abundant elemental constituents. At present, perovskite solar cells have been ushered in a new era of renewed efforts towards increasing the efficiency and lowering the cost of solar cells. Recently, Perovskite solar cells have reached an efficiency of nearly 20%. This technology combines the benefits of Dye Sensitized Solar Cells (DSSCs), Organic Photovoltaics (OPVs), and thin film solar cells. In this review, we have reported the brief prior art perspective of perovskite based solar cells, take a cognizance of the current state-of-the-art, highlight the challenges and the opportunities. This review also gives an overview on the impact of different hole transport materials (HTM), electron transport materials (ETM) and the role of Carbon nanomaterials as ETM, HTM and electrode materials.*

***Keywords:*** *Carbon nanomaterials; DSSCs; ETM; HTM; OPVs; Perovskites solar cells.*

## 1. INTRODUCTION

Conventional solar cells, which are used in rooftop applications, are based on single-crystal silicon and possess efficiency up to 25% efficient. Considerably more expensive solar cells based on GaAs (gallium arsenide) single crystals are ~29% and over 40% efficient in single and multijunction devices, respectively. They are used on satellites and in other space applications. Over the past 2 decades, solar cells based on thin-film polycrystalline materials, especially CdTe (cadmium telluride) and CIGS (copper indium gallium selenide), have emerged as a viable alternative to silicon cells with efficiencies exceeding 20%.

Solar cells are divided into few generations, depending on the composition and structure (Dobrzańska-Danikiewicz *et al.* 2011; Dobrzański *et al.* 2013)

- First generation solar cells are photovoltaic solar cells based on mono and polycrystalline silicon.
- Second generation solar cells like solar cells from first generation are based on p-n junction formed from doped semiconductors. These include the cell based on Cadmium telluride (CdTe), Copper selenide indium (CIGS) and amorphous silicon (a-Si).
- Third generation solar cells are photovoltaic cells based on organic compounds which do not have typical p-n junction as in first and second generation solar cells. These include dye-sensitized solar cells such as DSSC, tandem solar cells and volume solar cells.
- Fourth generation solar cells are Quantum dot sensitized solar cells (QDSSC).

Organic/ Inorganic hybrid perovskites have a high absorption coefficient, so a thin of perovskite light absorber is sufficient as a photo-active layer in Perovksite solar cells (PrSCs). Therefore, the devices can be thin and light (Stranks *et al.* 2013). Because of these advantages and high PCE, PrSCs have the potential to replace conventional Si solar cells to provide portable, mobile and wearable power sources.

***S. Karthikeyan Tel. no: +919442264501***
***Email:*** *environkarthi@gmail.com*

## 2. IDEOLOGY OF ORGANIC/INORGANIC PEROVSKITE MATERIALS

Recently, the perovskite sensitizer has attracted great attention due to its superb light-harvesting characteristics and it is composed of inexpensive and earth abundant materials (Kojima *et al.* 2009; You *et al.* 2014). Perovskite solar cell technology has been recognized as one of the biggest scientific breakthroughs of 2013 by the editors of Science and Nature (Nam-Gyu Park, 2015**)**. Perovskite was first used as a sensitizer based on dye-sensitized Gratzel solar cells in which molecular dye was replaced by perovskite.

Perovskite, named after the Russian mineralogist L. A. Perovski, has a specific crystal structures that have originated from the calcium titanium oxide mineral ($CaTiO_3$). Generally, perovskite structures have an $ABX_3$ formula, where cation A is occupied in a cubo-octahedral site and it is located at the corner positions (0, 0, 0), cation B is occupied in an octahedral site at the centre (1/2, 1/2, 1/2) and monovalent anion X is at the centre of the six planes (1/2 ,1/2 ,0) assuming them as the idealized cubic unit cell. Fig.1 shows the schematic diagram of cubic perovskite crystal structure. The most widely used component materials for PrSCs are organic molecule cations based on amine at A sites (e.g., $C_nH_{2n+1}NH_3^+$, $HC(NH_2)_2^+$), metal cations (e.g., $Pb^{2+}$, $Sn^{2+}$, $Cu^{2+}$) at B sites, and halide anions ($Cl^-$, $Br^-$, $I^-$) at X sites (Kim *et al.*2016).

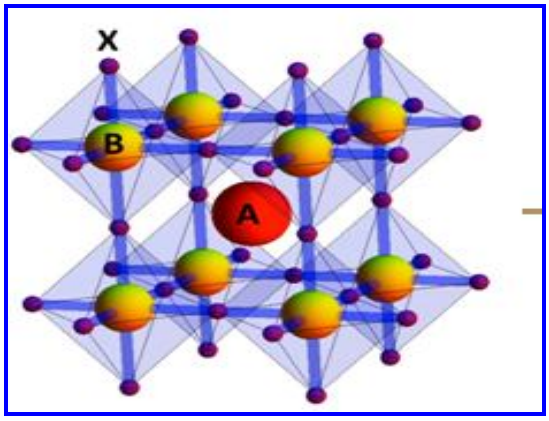


**Fig. 1: Schematic diagram of cubic perovskite crystal structure.**

In methylammonium lead iodide ($CH_3NH_3PbI_3$), the A-site cation is $CH_3NH_3^+$ and the B-site cation is $Pb^{2+}$, methylammonium cation is suitable for lead halide perovskite because its ionic radius is 1.8 A°. The absorption coefficient of $CH_3NH_3PbI_3$ was estimated to be $1.5 \times 10^4$ $cm^{-1}$ at 550 nm, indicating that the penetration depth for 550 nm light is only 0.66 mm. At 700 nm, the absorption coefficient was $0.5 \times 10^4$ $cm^{-1}$, corresponding to a penetration depth of 2 µm. Most of the incoming light can be absorbed by the perovskite within a thin layer of about 2 µm, which is suitable as a sensitizer for high efficiency solid-state sensitized solar cells (Nam-Gyu Park, 2015).

Miyasaka and coworkers in 2009 reported the first perovskite sensitized solar cells in which $CH_3NH_3PbI_3$ and methylammonium lead bromide ($CH_3NH_3PbBr_3$) were used as the photo sensitizers and in combination with the iodide/triiodide ($I^-/I_3^-$)-based liquid electrolyte wherein PCEs of 3.8% and 3.1% were obtained for the triiodide and tribromide based perovskite solar cells respectively. Later, in 2011, the titania surface and perovskite processing were optimized, which gave a PCE of 6.5% with the $CH_3NH_3PbI_3$ based iodide liquid electrolyte solar cell. PCE of 9.7% was achieved by Kim *et al.* (2012) in which the liquid electrolyte was replaced with a solid electrolyte. Liu *et al.* (2013) developed a sequential deposition method for the formation of the perovskite pigment within the porous metal oxide film and achieved a high PCE of 15% which also considerably increased the reproducibility of cell performance. Similarly solar to electrical PCE of 15.4% has been achieved by incorporating vapor deposited perovskite as the absorbing layer in a simple planar heterojunction (p-i-n) solar cell. At the end of 2013, the architectures of the meso-superstructured solar cell (MSSC) were optimized and a PCE of up to 15.9%, short circuit current density ($J_{sc}$) = 21.5 mA / $cm^2$, open circuit voltage ($V_{oc}$) =1.02 V and fill factor (FF) = 0.71 were achieved in an all low temperature processed solar cell, which is considered as the highest reported efficiency amongst perovskite based solar cells (Wojciechowski *et al.* 2014).

A typical perovskite solar cell is composed of three major components with (1) a n-type semiconductor such as $TiO_2$ which serves as a gallows for electron transport (2) a methylammonium lead halide ($MAPbX_3$) perovskite based light absorber material and (3) a hole transport material (HTM) which is interfaced with the $MAPbX_3$ material for charge separation and subsequent hole transport and two electrodes. The performance of a PrSCs depends on the light harvesting efficiency of the light absorber material, the charge separation efficiency at the interface of $MAPbX_3$/HTM and the charge transport efficiency in both the HTM and $MAPbX_3$ layer (Cai *et al.* 2015). The perovskite layer absorbs light to generate charges that are driven to be separated and transported by the built-in electric field between the two electrodes; this is followed by injection of the electrons into the conduction band of the $TiO_2$ layer and of the holes into the hole transport layer; they are then collected by the electrodes (Kim *et al.* 2012). $MAPbX_3$ (X = Cl, Br, I) as the most successful perovskite materials exhibits the most attractive properties of ideal Photo voltaics (PV) absorbers:

1. Strong optical absorption due to s-p anti-bonding coupling.
2. High electron and hole mobilities and diffusion lengths.
3. Superior structural defect tolerance and shallow point defects.
4. Low surface recombination velocity and benign grain boundary effects (Snaith *et al.* 2007; Wan-Jian Yin *et al*. 2014)

## 3. PLANAR HETEROJUNCTION STRUCTURED CELLS

Planar heterojunction (PHJ) perovskite solar cells (PrSCs) can provide a method to fabricate flexible and tandem PrSCs. Various studies on PHJ PrSCs have focused on engineering aspects of the perovskite film as a photo-active layer to make it favourable for solar cells (Liang *et al*. 2014; Song *et al.* 2015) but studies on interlayer engineering of PrSCs are relatively lacking. PHJ PrSCs with high $V_{oc}$, high $J_{sc}$ and high FF can be achieved by using appropriate interfacial layers between the electrodes and perovskite light absorber. In order to maximize the built-in potential of the device and to facilitate charge transfer from perovskite to interfacial layers, the PHJ PrSCs should use a hole extraction layer (HEL) and an electron extraction layer (EEL) with well-matching ionization energy (IE) and electron affinity (EA) respectively, as compared to those of perovskites (Schulz *et al.* 2015; Wang *et al.* 2015). The use of interfacial layers with high electrical conductivity is favourable to make efficient charge transport and extraction to each electrode. Snaith *et al.* (2013) demonstrated flexible p-i-n PHJ PrSCs on PET/ITO substrates as shown in fig.2 (FTO / PEDOT:PSS / $MAPbI_{3-x}Cl_x$ / PCBM / $TiO_x$ / Al), the devices had a PCE = 6.3%. Around the same time, Kelly *et al.* (2014) reported flexible n-i-p PHJ PrSCs and the devices were completed on PET/ITO substrates as well with the ITO / ZnO / $MAPbI_3$ / spiro-OMeTAD/Ag structure with the PCE of 10.2%.

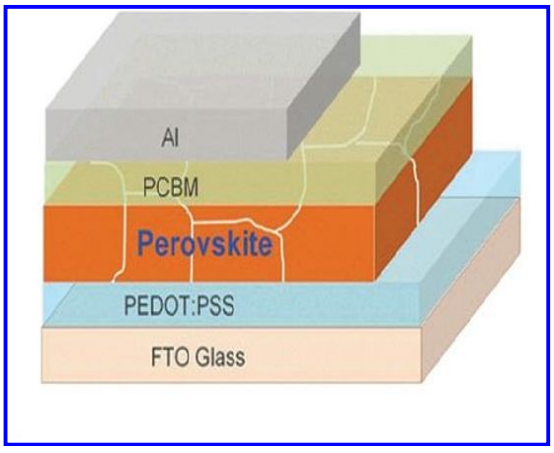


**Fig. 2: The device architecture of p-i-n Planar heterojunction PrSCs**

Chen *et al.* (2014) and Liu *et al.* (2014) has demonstrated a simplified perovskite solar cell with a planar thin-film "p-i-n" architecture in which $TiO_2$ and ZnO p-i-n structures were employed to obtain PCEs of 12.1% and 15.7%, respectively. But it remains a challenge to determine whether meso-structure is essential for the highest efficiencies or the thin-film p-i-n can lead to a superior technology.

## 4. HYBRID PEROVSKITE SOLAR CELLS

Lee *et al*. in 2012 fabricated hybrid PrSCs using a meso-superstructured organometal halide perovskite and obtained a power conversion efficiency of 10.9%, which triggered a lot of attention in the solar cell research community. Poly (3-hexylthiophene)/Phenyl-$C_{61}$-butyric acid methyl ester (P3HT/PCBM) blend has been extensively explored for inorganic photovoltaic applications. P3HT was replaced with $CH_3NH_3PbI_3$ as photoactive layer in planar heterojunction solar cell achieving a PCE of 3.9% (Liu *et al.* 2013). Better wettability was achieved with Poly(3,4-ethylenedioxythiophene):poly (styrenesulfonate) PEDOT: PSS coated ITO substrate with dimethylformamide (DMF) solution rather than coating perovskite active layer with $\gamma$-butyrolactone solution. Snaith *et al.* 2013 successfully reported that perovskite as top cell in a tandem cell configuration with existing technologies like crystalline silicone and thin film solar cells like CZTSSe, CIGS and CIS, has a potential to achieve $J_{sc}$ of 20 mA $cm^{-2}$ and $V_{oc}$ of 1.1V. Recently the concept of hybrid planar heterojunction cell incorporating 285 nm thick layer of $CH_3NH_3PbI_3$ was investigated in which active layer was sandwiched between hole transportin g poly (N,N'-bis(4-butylphenyl)-N,N'-bis(phenyl) - benzidine) (poly-TPD) layer (10 nm) and electron accepting PCBM layer (10 nm) resulting in a PCE of 12% (Abrusci *et al.* 2013).

Organic/Inorganic hybrid halide perovskite solar cells exhibit impressive competitiveness with other photovoltaic techniques due to their unique advantages:

(i) Low cost, earth abundance and easy preparation.
(ii) Near-perfect crystallinity at low temperature.
(iii) Large charge-carrier diffusion length of approximately 1 μm for mixed-halide perovskite ($CH_3NH_3PbI_{3-x}Cl_x$) thin films, which is 100 times higher than the other low-temperature solution processed thin films (Stranks *et al.* 2013).
(iv) Lower value of "loss-in-potential" in a solar cell, which allows the $V_{oc}$ of the best perovskite cells to be greater than 1.1 V (Snaith, 2010).
(v) Its bandgap can be tuned in the range of 1.48-2.23 eV by replacing the

methylammonium cation with the slightly larger formamidinium cation (Eperon *et al.* 2014) and part replacement of I with Br/Cl ions (Noh *et al.* 2013; Ball *et al.* 2013).

(vi) Perovskite materials are better than silicon at absorbing higher-energy blue and green photons (Service, 2013).

Meanwhile, perovskite materials also have some ineluctable disadvantages such as:

(i) perovskite materials are extremely sensitive to oxygen and water vapor, which reacts to break down the crystal structure and dissolves the salt like perovskite, respectively. The preparation of perovskite thin films should be performed in inert atmosphere.

(ii) It is challenging task to prepare large continuous films, which limits its scope for large scale production.

(iii) Lead in the most used perovskite solar cells is toxic and could leach out of the solar panel onto rooftops or the soil below.

(iv) Since there is a phase transition from tetragonal to cubic at 55 °C, the longer-term stability of perovskite solar cells has not been verified. There are reports of a few studies on storage lifetime but only limited on an operating cell (under illumination at the maximum power) for a sealed cell at 45 °C which showed a decrease in efficiency of less than 20% after 500 hrs (Burschka *et al.* 2013).

## 5. FLEXIBLE PEROVSKITE SOLAR CELLS

Low temperature solution processability of perovskite solar cells makes it possible to fabricate solar cells on flexible substrates. Fig.3 shows the device structure of low temperature processed perovskite solar cells. $CH_3NH_3PbI_{3-x}Cl_x$ as active layer with PEDOT: PSS and PCBM as hole-transporting and electron selective contacts, respectively, have been investigated in regular and inverted device architecture on an ITO coated polyethylene terephthalate (PET) substrate, achieving a PCE of 6.4% have been reported (Malinkiewicz *et al.* 2014). A higher PCE of 10.2% was achieved using device structure of ITO/ZNO (25 nm)/ $CH_3NH_3PbI_3$ / 2, 2',7,7'-tetrakis (N,N-p-dimethoxy-phenylamino)-9,9'-spirobifluorene (spiroMeOTAD)/ Ag, fabricated using low temperature solution processing techniques (Docampo *et al.* 2013). ITO coated polyethylenaphthalate (PEN) substrate has been used to demonstrate a wearable perovskite based energy source and reported PCE of 12.2% with only 5% loss over 1000 bending cycles of radius 10 mm (Kim *et al.* 2015).

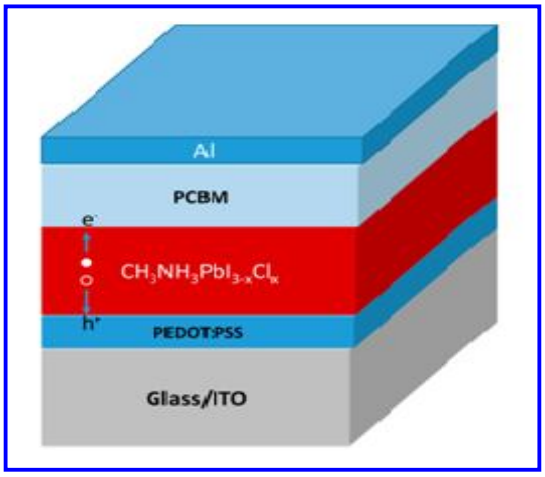


**Fig. 3: Device structure of low-temperature processed perovskite solar cell.**

The brittleness of FTO and ITO limits the development of flexible PrSCs. Therefore, finding a way to replace the conventional FTO and ITO electrodes with a transparent flexible electrode is a major requirement for development of flexible PrSCs. Although several papers have reported PrSCs that use flexible transparent conducting electrodes instead of FTO or ITO, their corresponding PCEs of the flexible devices were lower than rigid devices due to inferior electrical and optical properties of flexible electrodes (Roldan-Carmona *et al.* 2014; Poorkazem *et al.* 2015). Various kinds of flexible transparent conducting electrodes like PEDOT: PSS, graphene (Kim *et al.* 2014) carbon nanotubes (Han *et al.* 2012) and silver nanowires (Lee *et al.* 2014) have been successfully reported with the goal of enhancing compatibility with flexible PrSCs to replace conventional metal oxide brittle electrodes.

## 6. INFLUENCE OF HOLE AND ELECTRON TRANSPORT LAYERS

Organo lead halide perovskite is an ionic crystal; it easily dissolves in a polar solvent, hence it is not suitable for liquid electrolyte based sensitized solar cell. The tumbling block in the liquid electrolyte based perovskite solar cell was the dissolution and decomposition of perovskite in the liquid electrolyte. Resultantly the solar cells exhibited poor stability and would thereby degrade within minutes. Kojima and coworkers in 2006 found the solution to this problem in adoption of solid state hole transport material in place of liquid. Methylammonium trihalogen plumbates being relatively insoluble in nonpolar organic solvents, paved the way for realizing first perovskite sensitization and made subsequent infilling with the organic hole conductor possible. This prompted Murakami, Miyasaka and Park in collaboration with Gratzel and his coworkers to develop solid-state perovskite solar cells employing 2, 2',7,7'-tetrakis (N,N-p-dimethoxy-phenylamino)-

9,9'-spirobifluorene (spiro-OMeTAD) as the hole transporter (Im *et al.* 2011) with maximum full sun power conversion efficiencies of 10% (Hardin *et al.* 2012). The Chemical structure of spiro-OMeTAD is shown in fig. 4. Improvement in PCE was achieved in 2013, where 12.3% efficiency was reported using a perovskite sensitizer and poly-triarylamine (PTAA) as HTM and a higher efficiency of 14.1% was obtained by the National Renewable Energy Laboratory (NREL) (Noh *et al.* 2013). Organic HTMs have some unique advantages as compared to the inorganic hole conductors, such as the solution-processability, infinite variety, good stability, low-cost, environment-friendly, easy fabrication, tenability of electronic properties and mechanical flexibility.

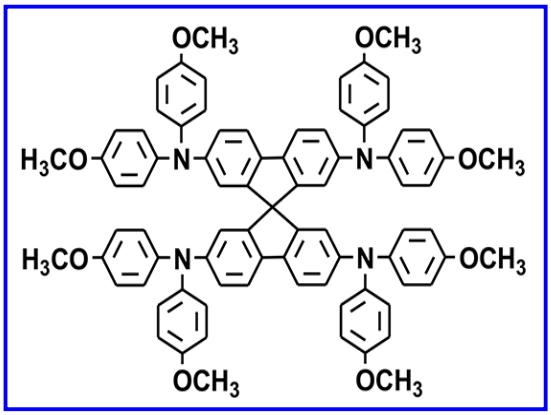


**Fig. 4: Chemical structure of spiro-OMeTAD**

PEDOT:PSS was also employed as an HTM (substrate/ITO/PEDOT:PSS/$CH_3NH_3PbI_{3-x}Cl_x$/PCBM/Al), where PEDOT:PSS and PCBM are used as hole and electron transport layers, respectively as shown in fig.5. Such architecture allowed the fabrication of a flexible perovskite solar cell with a PCE of 9.2% by replacing the rigid glass/ITO substrate with a flexible PET/ITO substrate as shown in fig.6. (You *et al.* 2014). $CH_3NH_3PbBr_3$ in a mesoporous $TiO_2$ with poly[N-9-hepta-decany l-2, 7-carbazole-alt-3,6-bis-(thiophen-5-yl)-2,5-dioctyl-2,5-dihydropyrrolo [3,4-]pyrrole-1,4-dione] (PCBTDPP) as HTM layer generated a $V_{oc}$ of 1.2V (Edri *et al.* 2013). Whilst the employment of P3HT as HTM, $V_{oc}$ got reduced to 0.5V. When considering electron injection from the photoactive layer to mesoporous titania, $V_{oc}$ is determined by difference in the Fermi level of $TiO_2$ and the (Highest Occupied Molecular Orbital) HOMO level of the HTM (Qiu *et al.* 2013). PCBTDPP based device afforded enhanced light filtering and stronger chemical interaction effecting charge recombination and an up-shift of Fermi level resulting in a high $V_{oc}$. Faster recombination in P3HT resulted in electron lifetime being one order of magnitude lower than spiro-MeOTAD in $TiO_2$ /$CH_3NH_3PbI_3$/HTM system (Cai *et al.* 2013). Perovskite sensitized solid state solar cells using spiro-OMe-TAD, P3HT and 4-(diethylamino) benzaldehyde diphenylhydrazone (DEH) as HTMs have achieved with a light to electricity power conversion efficiency of 8.5%, 4.5%, and 1.6%, respectively, under AM 1.5G illumination of 1000 $W/m^2$. The electron lifetime ($\tau_e$) in these devices are in the order spiro-OMeTAD > P3HT > DEH, while the charge transport time ($t_{tr}$) is rather similar. The difference in $\tau_e$ can therefore explain the lower efficiency of the devices based on P3HT and DEH. The nature of the HTM is essential for charge recombination and elucidates that finding an optimal HTM for the perovskite solar cell involves controlling the perovskite/HTM interaction (Dongqin Bi *et al.* 2013).

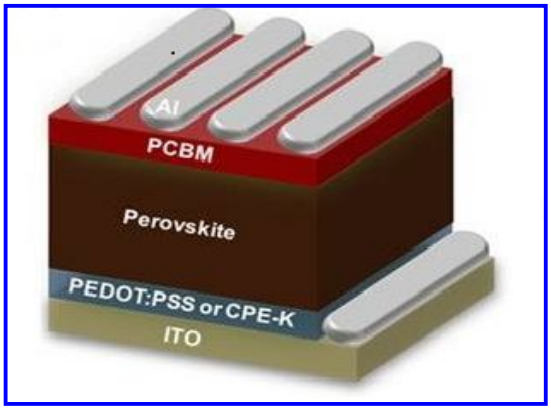


**Fig. 5: Device structure of flexible perovksite solar cell on PET/ITO substrate**

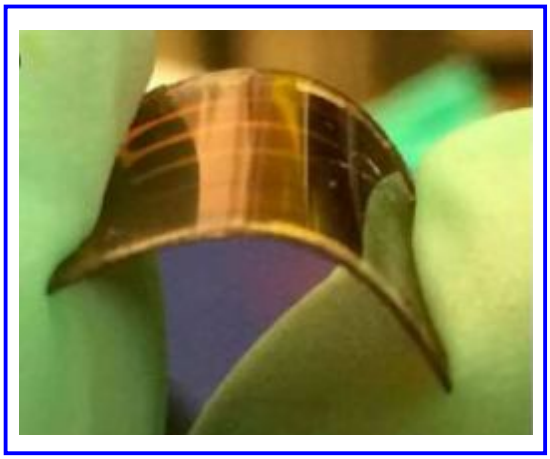

**Fig. 6: Photo image of flexible perovksite solar cell on PET/ITO substrate**

The widely used organic hole conductors including spiro-OMeTAD and P3HT may represent a potential hurdle to the future commercialization of this type of solar cell because of their relatively high cost. To this end, a $CH_3NH_3PbI_3$ perovskite-sensitized solar cell utilizing an inexpensive, stable, solution-processable inorganic CuI as the hole conductor has been demonstrated (Christians *et al.*

2014). It was also demonstrated that the solution-processable p-type direct bandgap semiconductor $CsSnI_3$ with perovskite structure can also be used for hole conduction replacing a liquid electrolyte (Chung *et al.* 2012). PEDOT:PSS is commonly used as a hole transport layer, but it is generally considered as an unstable transport layer for organic devices due to its hydrophilic and acidic nature (DeJong *et al.*2000). The stable p-type metal oxide $NiO_x$ was used to overcome this issue and improve device stability. The device structure of all metal oxide based perovskite solar cell is shown in fig. 7. This consists of glass/ITO/$NiO_x$/perovskite ($CH_3NH_3PbI_3$)/ZnO/Al, where the $NiO_x$ and ZnO act as the hole and electron transport layers, respectively. $NiO_x$ has been demonstrated as an efficient hole conductor in the $CH_3NH_3PbI_3$ where a PCE of 9.5% was achieved with nanocrystalline $NiO_x$ layer (Wang *et al.*2014). On exposure to light, charge carriers are generated in the perovskite layer and electrons and holes are subsequently collected by their respective contacts, ZnO and $NiO_x$. Meanwhile, Graphene oxide (GO) is also employed as a hole conductor in inverted planar heterojunction perovskite solar cells employing $CH_3NH_3PbI_{3-x}Cl_x$ as absorber and GO as hole conductor as shown in fig. 8, achieves a PCE of 12.4%. The common PEDOT:PSS-based device results in an efficiency of 9.26%, which is extremely improved from the original 2.64% efficiency of the device without a hole conductor (Zhongwei Wu *et al.* 2014).

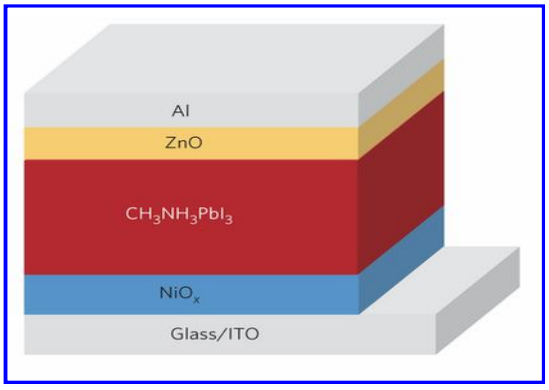


**Fig. 7: Device structure consisting of glass/ITO/$NiO_x$/ $CH_3NH_3PbI_3$/ZnO/Al.**

The first use of hybrid perovskite absorbers in photovoltaic cells is based on the typical structure of a dye-sensitized solar cell, where the perovskite absorber is self-assembled within the gaps of a porous $TiO_2$ layer formed by sintering nanoparticles. The typical configuration of this type of perovskite - based solar cell is FTO/dense$TiO_2$/mesoporous$TiO_2$/perovskite/spiro-OMeTAD/electrode as shown in fig.9. In this structure, perovskite materials are deposited onto mesoporous $TiO_2$, which is used to facilitate electron transport between the perovskite absorber and the FTO electrode (Gratzel *et al.* 2013). Solar cells with new architectures in which the mesoporous $TiO_2$ was successfully replaced with an insulating porous $Al_2O_3$ scaffold indicated that perovskites have a broader potential than just being used as sensitizers, as they are able to transport both electrons and holes between cell terminals (Lee *et al.* 2012). Intriguingly, the PCE of such a Meso-super structured solar cell (MSSC) unexpectedly reached 10.9% with a high $V_{oc}$ of 0.98 V (~0.2-0.3 V higher as compared to the mesoporous $TiO_2$), which gives great promise for significant futuristicenhancements in efficiency. It also suggests that original components of the DSSCs no longer remain. Recently, the PCE of MSSC based on perovskite has been further improved up to 15.9% (Wojciechowski *et al.* 2014).

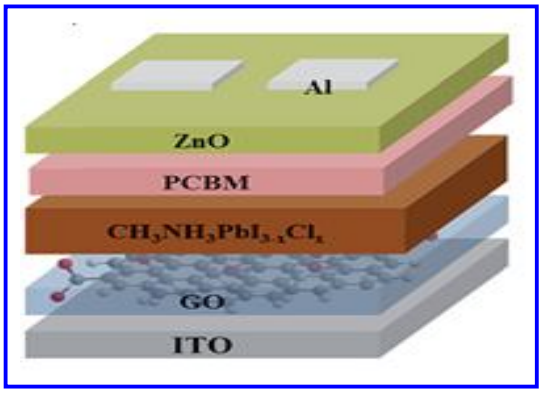


**Fig. 8: Schematic diagram of ITO/GO/ $CH_3NH_3PbI_{3-x}Cl_x$/PCBM/ZnO/Al device structure.**

The pyrene derivatives were employed as HTMs in fabricating mesoporous$TiO_2$/$CH_3NH_3PbI_3$/ HTM / Au solar cells. The pyrene based derivative Py-C exhibited $J_{sc}$ of 20.2 mA/cm$^2$, $V_{oc}$ of 0.886 V and FF of 69.4 % under an illumination of 1 sun (100 mW/cm$^2$), resulting in an overall efficiency of 12.4 % (Jeon *et al.* 2013). Several literature review on different device architecture and Photovoltaic parameters of different HTMs are represented in table 1.

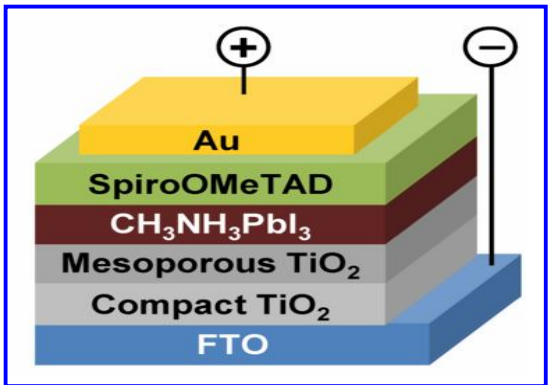


**Fig. 9: Schematic illustration of photovoltaic cell using $CH_3NH_3PbI_3$ and mesoporous $TiO_2$.**

**Table 1. Device architecture and photovoltaic parameters of different hole transport materials (HTM)**

| Pervoskite | Structural Design | HTM | $V_{oc}$ (V) | $J_{sc}$ ( mA $cm^{-2}$) | FF (%) | PCE (%) | References |
|---|---|---|---|---|---|---|---|
| $MAPbI_{3-x}Cl_x$ | ITO/PEIEl/Y:$TiO_2$/$MAPbI_{3-x}Cl_x$/ Spiro-OMeTAD/Au | Spiro-OMeTAD | 1.13 | 22.75 | 75.01 | 19.3 | Zhou *et al.* 2014 |
| $MAPbI_3$ | ITO/PEDOT:PSS/HTM/ $MAPbI_3$/PCBM/LiF/Ag | PCDTBT | 1.03 | 15.9 | 66 | 10.9 | Lin *et al.* 2015 |
| $MAPbI_{3-x}Cl_x$ | ITO/HEL/$MAPbI_{3-x}Cl_x$/$C_{60}$/Ag | Spiro-TTB | 0.970 | 14.9 | 63 | 9.1 | Polander *et al.* 2014 |
| $MAPbI_3$ | ITO/HEL/$MAPbI_3$/$PC_{61}BM$/Al | SOHEL | 0.982 | 16.7 | 70.5 | 11.7 | Lim *et al.* 2014 |
| $MAPbI_3$ | ITO/HEL/$MAPbI_3$/$PC_{61}BM$/ | Poly-TPD | 0.99 | 20.1 | 69.55 | 13.78 | Zhao *et al.* 2015 |
| $MAPbI_3$ | FTO/$TiO_2$/$MAPbI_3$/spiro-OMeTAD/Au | Spiro-OMeTAD | 1.05 | 19.8 | 64 | 13.7 | Yella *et al.* 2014 |
| $MAPbI_3$ | ITO/PEDOT:PSS/$MAPbI_3$/ $PC_{61}BM$/$C_{60}$/BCP/Al | PEDOT: PSS | 0.99 | 19.6 | 79.3 | 15.4 | Xaio *et al.* 2014 |
| $MAPbI_3$ | ITO/ZnO NP/$MAPbI_3$/P3HT/Ag | P3HT | 0.94 | 17 | 62 | 11.8 | Liu *et al.* 2014 |
| $MAPbI_{3-x}Cl_x$ | ITO/GO/$MAPbI_{3-x}Cl_x$/$PC_{61}BM$/ ZnO/Al | GO | 1.00 | 17.46 | 71 | 12.4 | Wu *et al.* 2014 |
| $MAPbI_{3-x}Cl_x$ | FTO/$WO_x$/$MAPbI_{3-x}Cl_x$/spiro-OMeTAD/Ag | Spiro-OMeTAD | 0.71 | 21.77 | 58 | 8.99 | Wang *et al.* 2015 |

$MAPbX_3$ based perovskites have been found to exhibit multiple phases as a function of temperature and composition. These different phases possess dramatically different electrical/optical properties as well as stability. Stoumpos *et al.*(2013) showed that $MAPbI_3$ exhibited an α-phase, δ-phase, and γ-phase with transition temperatures of 400 K, 333 K, and 180 K, respectively as shown in fig.10. In general, the δ-phase $MAPbI_3$ is used as the solar cell absorber because of its thermodynamically stable nature at room temperature and its increased absorption coefficient (>26 $mm^{-1}$) and conductivity, in contrast to the α-phase.

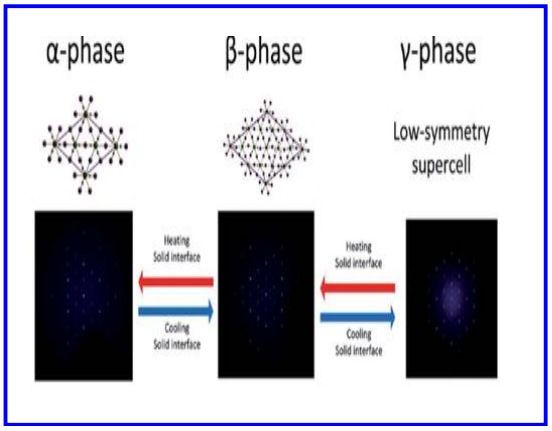


**Fig. 10: Phase transition of perovskite materials.**

Besides perovskites the transporting layers, including the ETL like $TiO_2$ and PCBM and HTL like spiro-OMeTAD and PEDOT: PSS also cause the instability of perovskite solar cells. The $TiO_2$ layer is sensitive to ultraviolet light and PCBM is not stable in air. For HTL, the use of spiro-OMeTAD required an additive like 4-ter[tbutylpyridine] (tBP), which can react with perovskite materials with regard to PEDOT:PSS its acidic nature also becomes a concern for the long-term stability of solar cells (Tze-Bin Song *et al.* 2015).

Low conductivity (~$10^{-5}$ $Scm^{-1}$) of HTM is the major reason for low FF of perovskite solar cells which can be remedied by doping the HTM with protic ionic liquids (PILs) as effective p-type codopant. Lithium salts added to spiro-MeOTAD increases the hole conductivity in spiro-MeOTAD (Snaith *et al.* 2006).

In a typical perovskite solar cell, a several hundred nanometer thick absorber layer, either with or without mesoporous scaffold is sandwiched between the electron transport layer (ETL) and hole transport layer (HTL). Upon the absorption of incident photons, carriers are created in the absorber that travels through ETL, the electrodes and in between each interface. To increase the PCE, it is essential to precisely manipulate carriers along the entire pathway from the absorber to both electrodes.

In contrast to the majority of perovskite solar cells, based on FTO and ITO electrodes further modification was accomplished with polyethyleneimine ethoxylate (PEIE) (Zhou *et al.* 2012), a polymer containing simple aliphatic amine groups to reduce the work function of ITO. Burschka *et al.* (2013) used Yttrium doped $TiO_2$ (Y-$TiO_2$) as ETL to enhance electron extraction and transport, further cobalt and lithium co-doped spiro-OMeTAD and gold were used as the HTL and electrode for hole extraction. To enhance the carrier concentration of the electron transport channel in the device, doping with $TiO_2$ ETL was done alongwith modifying the ITO electrode that reduced its work function and produced a PCE of 19.3%. The $TiO_2$-based cell produced a $J_{sc}$ of 19.9 mA/cm$^2$, $V_{oc}$ of 1.06 V and FF of 65.44%, yielding a PCE of 13.8%, whereas the Y-$TiO_2$ based device had $J_{sc}$ of 22.8 mA/cm$^2$ and a PCE of 16.5%.

Min *et al.* (2014) successfully fabricated efficient p-i-n $CH_3NH_3PbI_{3-x}Cl_x$ based Hybrid solar cells using a metal oxide (ZnO) and an n-type small molecule perylene diimides (PDI) as the core and amino perylene diimides **(**PDIN**)** or amino N-oxide perylene diimides (PDINO**)** as ETLs. Both, ZnO and PDINO layers can effectively modify the PCBM/Ag interface and increase the $V_{oc}$ values from 0.85 to 0.95 V. Although the PCBM/ZnO/Ag device shows an improved PCE of 11.3% as compared to the controlled PCBM/Ag device (10.0%), its $J_{sc}$ value is slightly reduced either due to optical effects or may be due to a reduced current collection from the rougher interface or due to a combination of both mechanisms. The PCE was further improved to 14.0% under AM 1.5G illumination by inserting a well conducting n-type PDINO layer between PCBM and the Ag electrode. Notably, PDINO-based devices showed prominent PCEs over 13% within a wide range of the PDINO thicknesses (5-24 nm). PDINO offers the desired electronic levels for electron extraction, gives homogeneous and smooth films with a good collection probability and successfully prevents the diffusion of Ag ions to the semiconductor interface. PDINO based devices also show the higher device stability as opposed to those devices with PCBM/Ag and PCBM/ZnO/Ag cathodes. The ability to obtain high efficiency and stability using PDINO expands the present range, rather limited, of available cathode interface layers for pero-HSCs.

Chu *et al.* (2015) introduced solution-processable $MoO_3$ between ITO and PEDOT:PSS, and developed a device that had the ITO/ $MoO_3$/PEDOT:PSS/$MAPbI_3$/$C_{60}$/Bphen/Ag structure. The device showed better long term stability than the device with only PEDOT:PSS. Metal ions released from ITO due to damage by acidic PEDOT:PSS can diffuse into the inner layer of a device and degrade the device performance. However, insertion of $MoO_3$ seems to effectively prevent corrosion of ITO by PEDOT:PSS and consequent generation of undesirable species. After 10 days under ambient conditions, the PCE of the device with MoO3 degraded only 7%, whereas the device with only PEDOT:PSS failed completely. Furthermore, owing to increased hole collection efficiency, the device with $MoO_3$ showed a higher PCE of 12.78% than the device with only PEDOT:PSS HTL (PCE = 9.81%). In another approach, Yeo *et al.* (2015) replaced PEDOT:PSS with reduced graphene oxide (rGO) nanosheets as HTL and the replacement increased device stability as well as PCE. The longer half-lifetime of rGO device (B150 h) than the device with PEDOT:PSS (B50 h) under ambient conditions was attributed to rGO with nearly neutral properties, unlike PEDOT:PSS, which is acidic with few surface oxygen functionalities, rGO has inherent passivation ability against moisture and oxygen. Also, the device with rGO achieved a PCE of 10.8%, which was higher than a PCE of 9.14% of the device with PEDOT:PSS. These results were ascribed to the superior charge transport ability due to higher conductivity of rGO than PEDOT:PSS and better-aligned energy levels between rGO and the anode. Several literature review on different device architecture and photovoltaic parameters of different ETMs are represented in table 2.

In general, PrSCs consist of a transparent conductive substrate, an electron transport layer (ETL), an optional mesoscopic layer, a perovskite layer, a hole transport layer (HTL), and a metal cathode. In PrSCs, $TiO_2$ is commonly used as an electron transport material. $TiO_2$ exhibits certain electrical conductivity only after the formation of nanocrystallites. Therefore, $TiO_2$ crystallite formation at a low temperature is the key point in the preparation of $TiO_2$ ETM. Snaith *et al.* (2014) combined graphene and $TiO_2$ as ETL after preparing $TiO_2$ nanoparticles. The temperatures adopted were 150 °C or less and a remarkable PCE was achieved. However, the preparation of low temperature $TiO_2$ ETL is relatively complicated because $TiO_2$ crystallization is difficult. Although ZnO possesses high electron mobility (>200 cm$^2$ $V^{-1}s^{-1}$) (Zhang *et al.* 2009; Shi *et al.* 2013), it can also be used as ETL in PrSCs, (Liu *et al.* 2014). ZnO is chemically unstable and usually reacts with weak acids or weak bases. Thus developing new technology or new functional materials is urgently needed for the preparation of ETL at low temperature with simple processes.

Tungsten oxides ($WO_x$) are chemically stable semiconductors with wide bandgaps (2 to 3 eV) (Wang *et al.* 2012) and higher electron mobility ($10^{-20}$ cm$^2$ $V^{-1}$ $s^{-1}$) (Gillet *et al.* 2004). These appealing properties enable efficient transportation of

photogenerated electrons. The $WO_x$ ETL exhibited excellent light transmittance and significantly higher electrical conductivity compared with conventional $TiO_2$. In addition, subsequent photo−luminescence decay indicated a faster kinetic process of charge transfer at the $WO_x$ ETL/perovskite interface. These advantages enabled $WO_x$-based PrSCs to provide higher $J_{sc}$. Finally, a PCE of ~8.99% was achieved by $WO_x$ based PrSCs, which is comparable to that of the $TiO_2$ based PrSCs with PCE of 8.78%. It is believed that the photovoltaic performance of $WO_x$ based PrSCs can be further improved through some strategies of suppressing the interface charge recombination.

Studies on ETLs of p-i-n PHJ PrSCs have also been reported. PCBM, the popular ETL, has been doped with graphdiyne, a novel two-dimensional carbon material (Li *et al.* 2015). While the electron mobility of a unipolar device with pure PCBM was 2.98 x $10^{-4}$ $cm^2$ $V^{-1}$ $s^{-1}$, it was increased to 5.32 x $10^{-4}$ $cm^2$ $V^{-1}$ $s^{-1}$ in the device that used graphdiyne doped $PC_{61}BM$. The improvement in electron mobility resulted from good electrical characteristics of graphdiyne owing to its carbon network structure with delocalized p-systems. In addition, the device with $PC_{61}BM$: graphdiyne exhibited less charge recombination because of the better coverage of the EEL and the interfacial contact with the perovskite surface than undoped $PC_{61}BM$. Due to the increased electrical conductivity of the ETL, the device achieved a PCE= 14.8%, which was higher than PCE = 13.6% of the device with pristine $PC_{61}BM$. authors presented a clear correlation between the charge transporting properties of EELs [indene-$C_{60}$bisadduct ($IC_{60}BA$), $PC_{61}BM$ and $C_{60}$] and device performance. Electron mobilities of the fullerene derivatives were obtained from FETs based on each fullerene derivative. The gradual increase in electron mobility from ($IC_{60}BA$) (6.9 x $10^{-3}$ $cm^2$ $V^{-1}$ $s^{-1}$), to $PC_{61}BM$ (6.1 x $10^{-2}$ $cm^2$ $V^{-1}$ $s^{-1}$), to $C_{60}$ (1.6 x $cm^2$ $V^{-1}$ $s^{-1}$) was attributed to increased conjugation and dense packing of $C_{60}$ owing to the lack of bulky side-chains. Due to this reason, the device with $C_{60}$ as an ETL achieved the highest $J_{sc}$ = 21.07 mA $cm^{-2}$ and PCE = 15.44%; the device with $PC_{61}BM$ had a $J_{sc}$ =18.85 mA $cm^{-2}$ and PCE = 13.37%, and the device with $IC_{60}BA$ had a $J_{sc}$ = 11.27 mA $cm^{-2}$ and PCE = 8.06%. These results indicate that an ETL with good electrical conductivity of carbon nanomaterials promotes efficient charge transport in a device and increase its PCE.

**Table 2. Device architecture and photovoltaic parameters of different electron transport materials (ETM)**

| Pervoskite | Structural Design | ETM | $V_{oc}$ (V) | $J_{sc}$ (mA $cm^{-2}$) | FF (%) | PCE (%) | References |
|---|---|---|---|---|---|---|---|
| $MAPbI_{3-x}Cl_x$ | ITO/PEDOT:PSS/ $MAPbI_{3-x}Cl_x$/$PC_{61}BM$/PEIE/Ag | $PC_{61}BM$ | 0.899 | 17.32 | 77.1 | 12.01 | Zhang *et al.* 2014 |
| $MAPbI_3$ | ITO/TiOx/PC61BM/WS-$C_{60}$/$MAPbI_3$/P3HT/$MoO_x$/Al | $PC_{61}BM$ | 0.95 | 27.4 | 56.3 | 14.6 | Liu *et al.* 2015 |
| $MAPbI_{3-x}Cl_x$ | ITO/PEDOT:PSS/ $MAPbI_{3-x}Cl_x$/$PC_{61}BM$/PFN/Al | $PC_{61}BM$ | 1.05 | 20.3 | 80.2 | 17.1 | You *et al.* 2015 |
| $MAPbI_3$ | ITO/PEDOT:PSS/$MAPbI_3$/$PC_{61}BM$/$C_{60}$/BCP/Al | $PC_{61}BM$ | 0.99 | 19.6 | 79.3 | 15.4 | Xaio *et al.* 2014 |
| $MAPbI_3$ | ITO/PEDOT:PSS/$MAPbI_3$/$PC_{71}BM$/Ag | $PC_{71}BM$ | 0.87 | 18.66 | 75 | 12.22 | Paek *et al.* 2014 |
| $MAPbI_3$ | ITO/PEDOT:PSS/$MAPbI_3$/$PC_{71}BM$/Ca/Al | $PC_{71}BM$ | 1.05 | 19.98 | 78 | 16.31 | Chiang *et al.* 2014 |
| $MAPbI_3$ | ITO/PEDOT:PSS/$MAPbI_3$/$PC_{61}BM$/$C_{60}$/BCP/Al | $PC_{61}BM$ | 0.96 | 21.0 | 76 | 15.6 | Shao *et al.* 2014 |
| $MAPbI_3$ | FTO/PEDOT:PSS/$MAPbI_3$/$PC_{61}BM$/TIPD/Al | $PC_{61}BM$/TIPD | 0.89 | 22.57 | 64.5 | 12.95 | Li *et al.* 2015 |
| $MAPbI_{3-x}Cl_x$ | ITO/PEDOT:PSS/ $MAPbI_{3-x}Cl_x$/$PC_{61}BM$/PDINO/Ag | $PC_{61}BM$/PDINO | 0.95 | 18.8 | 78.5 | 14.0 | Min *et al.* 2015 |
| $MAPbI_{3-x}Cl_x$ | ITO/PEDOT:PSS/ $MAPbI_{3-x}Cl_x$/$PC_{61}BM$/PCBC/Al | $PC_{61}BM$/PCBC | 0.98 | 22.08 | 69.7 | 15.08 | Liu *et al.* 2015 |
| $MAPbI_3$ | ITO/PEDOT:PSS/$MAPbI_3$/$C_{60}$/ Bis-$C_{60}$/Ag | Bis-$C_{60}$ | 0.92 | 21.07 | 80 | 15.44 | Liang *et al.* 2015 |

The important roles of a fullerene based n-type layer in a p-i-n type PHJ solar cell was highlighted particularly with respect to electrical conductivity of the materials (Liang *et al.* 2015). The authors presented a clear correlation between the charge transporting properties of EELs [ indene-$C_{60}$ bisadduct ($IC_{60}$ BA), $PC_{61}BM$ and $C_{60}$] and device performance. Electron mobilities of the fullerence derivatives were obtained from FETs based on each fullerence derivative. The gradual increase in electron monility from $IC_{60}BA$ ($6.0 \times 10^{-3}$ $cm^2$ $V^{-1}$ $s^{-1}$), to PC61BM ($6.1 \times 10^{-2}$ $cm^2$ $V^{-1}$ $s^{-1}$), to C60 (1.6 x cm2 V-1 s-1) was attributed to increased conjugation and dense packing of C60 owing to the lack of bulky side-chains. Due to this reason, the device with C60 as an ETL achieved the highest authors presented a clear correlation between the charge transporting properties of EELs [indene-$C_{60}$bisadduct ($IC_{60}BA$), $PC_{61}BM$ and $C_{60}$] and device performance. Electron mobilities of the fullerene derivatives were obtained from FETs based on each fullerene derivative. The gradual increase in electron mobility from ($IC_{60}BA$) ($6.9 \times 10^{-3}$ $cm^2$ $V^{-1}$ $s^{-1}$), to $PC_{61}BM$ ($6.1 \times 10^{-2}$ $cm^2$ $V^{-1}$ $s^{-1}$), to $C_{60}$ ($1.6 \times$ $cm^2$ $V^{-1}$ $s^{-1}$) was attributed to increased conjugation and dense packing of $C_{60}$ owing to the lack of bulky side-chains. Due to this reason, the device with $C_{60}$ as an ETL achieved the highest $J_{sc}$ = 21.07 mA $cm^{-2}$ and PCE = 15.44%; the device with $PC_{61}BM$ had a $J_{sc}$ =18.85 mA $cm^{-2}$ and PCE = 13.37%, and the device with $IC_{60}BA$ had a $J_{sc}$ = 11.27 mA $cm^{-2}$ and PCE = 8.06%. These results indicate that an ETL with good electrical conductivity of carbon nanomaterials promotes efficient charge transport in a device and increase its PCE.

## 7. ROLE OF CARBON NANOMATERIALS IN PEROVSKITE SOLAR CELLS

Transparent graphene and carbon nanotubes (CNT) have been successfully employed as the counter electrode in DSSC devices (Kalaiselvan et al. 2016). Recently, transparent CNT networks have been proved to be good hole conductor for perovskite solar cells (Li *et al.* 2014). Incorporating one-dimensional [1-D] nanostructures into nanoparticulate films may overcome the problem by providing direct pathways for electron transport (Yu *et al.* 2009). CNTs a type of 1-D nanostructure, possess several unique properties including hollow and layered structures, a high aspect ratio, excellent electrical and thermal conductivity, high mechanical strength, and a large specific surface area (Burghard, 2005). Recent studies have revealed that CNTs have been utilized as electrodes due to their great chemical steadiness, high electrical conductivity, efficient charge collection, and low cost. In addition, other functionalities, including flexibility and high transparency, could be attained with the CNT electrodes. Li *et al.* (2014) exploited the laminated CNT networks as the top electrode of the semitransparent perovskite solar cells. Fig.11 represents the schematic diagram of semitransparent perovskite solar cell employing graphene based transparent top electrode. As the thickness of the CNT network film was very thin (20-50 nm), the optically transparent property was achieved and therefore the device could be illuminated from both the FTO and CNT sides. spiro-OMeTAD has been considered as one of the most successful HTMs, which has yielded the highest power conversion efficiencies in PrSCs. However, the low charge carrier mobility and lengthy synthetic route of spiro-OMeTAD may make it impractical for industrial applications in the future.

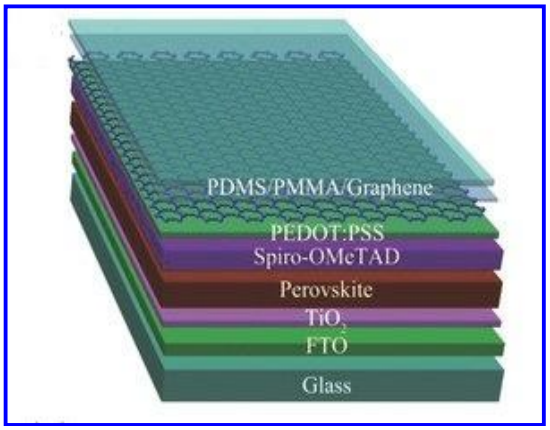


**Fig. 11: Schematic diagram of semitransparent perovskite solar cell**

The cell configuration of solid state perovskite solar cells based on Ti foil/$TiO_2$ nanotubes and carbon nanotubes is shown in fig 12. From bottom to top in sequence are Ti foil, TNT arrays loaded with perovskite absorber and CNT networks composite with spiro-OMeTAD. Dense TNT arrays grown on Ti foil by electrochemical anodization serve both as a scaffold for perovskite deposition and as an electron collector. CNT network acts as hole collector and transparent electrode. For better hole collection, the hole transport material spiro-OMeTAD is infiltrated in carbon nanotubes network. Light comes from CNT side, as indicated by arrow in fig. 12. Since Ti foil and CNT network are flexible materials, the integrated solar cell device is expected to show good flexibility. The CNT film is highly transparent with transmittance between 60% and 80% all over the $CH_3NH_3PbI_3$ absorption wavelength range from 300 to 800 nm. The CNT network is closely adhered to the perovskite by Van der waal force. From the magnified top morphology of CNT/perovskite shows that the bundled CNT networks are sparse with pores for light transmittance. In order to enhance hole collection in perovskite solar cells, spiro-OMeTAD are infiltrated into CNT networks by spin coating (Li *et al.* 2014).

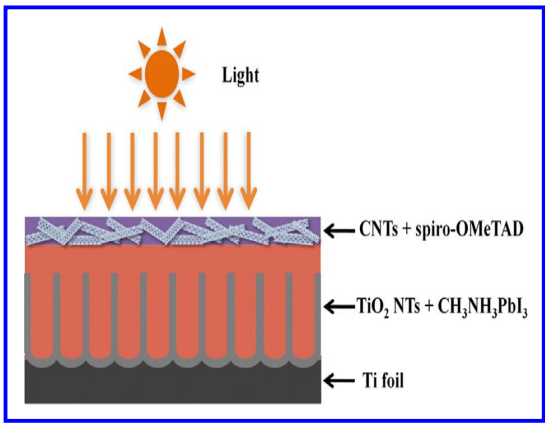


**Fig. 12: Schematic diagram of solid-state perovskite solar cells based on Ti foil/$TiO_2$ nanotubes and carbon nanotubes.**

The Ti foil/CNTs act as scaffold for perovskite loading and electron transport layer, while the transparent CNT top electrode acts as hole collecting layer and light transmission. With 25 µm Ti foil and $TiCl_4$ treatment to $TiO_2$ nanotube arrays, PCE up to 8.31% has been achieved. The solar cells on Ti foil maintain good performance after 100 mechanical bending cycles, indicating their excellent flexibility. Considering the high efficiency, good flexibility and simple fabrication technique, Ti foil/TNTs based flexible perovskite solar cells holds a promising future for roof-top photovoltaics and power sources for wearable devices. Carbon nanotubes are a p-type conducting material at ambient atmosphere with a reported work function between -4.95 and -5.05 eV at room-temperature condition (Shiraishi *et al.* 2001). PCE of 6.87% with a $V_{oc}$ of 0.88 V, $J_{sc}$ of 15.46 mA/cm$^2$, and fill factor of 0.51 under AM1.5 100 mW/cm$^2$ illumination was achieved by the best device of $CH_3NH_3PbI_3$/CNTs solar cells. Higher $V_{oc}$ and $J_{sc}$ might be due to better hole selectivity of CNTs than metallic Au, reducing the chance of interface recombination. The higher sheet resistance of CNT film (2-5 kΩ as measured by four-point probe) could explain the poorer fill factor. Therefore, removing impurities on the CNT surface to reduce the sheet resistance of the CNT film may improve the cell efficiency in the future. The $V_{oc}$ of the solar cell decreased with the decrease of incident light intensity; however, the FF improved at lower light illumination. The low thickness of CNT network films allows for the perovskite solar cells to be illuminated from both directions (Li *et al.* 2014).

Carbon nanotube networks provided a straightforward implementation of nanostructured hole collectors in P3HT:PCBM blend devices and resulted in as much as a 10% increase in the device power conversion efficiency from a 20% increase in the associated optimal active layer thickness, which was caused by improved $J_{sc}$ in the tested blend thickness range (Chang-Yong Nam *et al.* 2011). Perovskite solar cells with a flexible fiber structure were now prepared for the first time by continuously winding an aligned multiwalled carbon nanotubes (MWCNT) sheet electrode onto a fiber electrode.

## 8. FUTURE PROSPECTS

Although PrSCs exhibit attractive prospect, the stability problem and the environmental issue of the perovskite crystal will be a big limitation for the large-scale application. Therefore, future studies should focus on the development of low-cost, stable and environmental friendly light-harvesting materials. $CH_3NH_3PbI_3$ and mixed halide perovskite $CH_3NH_3PbI_{3-x}Cl_x$ are at the center of research into high efficiency perovskite solar cells. With these materials, a PCE of 20% have been achieved from single junction structures and a PCE of 29% is expected from tandem structures (Nam-Gyu Park, 2013). Higher efficiency is still possible through structural modification (Snaith, 2013), along with band gap tuning. Modification of the bond distance and/or angle of X-Pb-X in $CH_3NH_3PbX_3$ is one of strategies to tune band gap energy. More recently, a PCE approaching 30% was achieved from a single junction perovskite solar cell (Yin *et al.* 2014). Optimistic expectations for the perovskite solar cell are based on the superb opto-electronic property of organo metal halide perovskite material that is even better than high efficiency GaAs. Since the high $V_{oc}$ observed from organo metal halide perovskite is likely to be related to high internal photoluminescence quantum efficiency (Nayak *et al.* 2014), careful control of the luminescent property of perovskite could further improve $V_{oc}$, hence contributing to an even higher PCE. Finally, substitution of other elements for Pb (Ogomi *et al.* 2014) is one of the important tasks for environment friendly perovskite solar cells.

Low temperature solution processing assures low per watt cost and quick energy payback times. Device architectures ranging from p-i-n (Ball *et al.* 2013) to mesoporous to mesosuperstructure configuration throw wide open possibilities for incorporation of novel materials and synthesis approaches. The future may hold no scaffold pin planar configuration or the incorporation of other semiconductor materials for inert oxide scaffold. Use of materials with high mobility as HTM will further improve the FF while optimization of the interfaces and selection of HTM and ETM may push forward the efficiencies to higher values. Incorporation of narrow band gap perovskites and plasmonic light harvester may broaden the spectral response with better light harvesting. Interface engineering and introduction of self-assembled layers will reduce losses and improve efficiency. Understanding of the underlying photophysical phenomenon will further

help improving device structures and better selection of materials. Exploration of tandem cell configuration with perovskite based cell as the top cell will push forward the achievable efficacy limit further. With the tremendous amount of research effort under way, guided by the adherence to the issue of best practices (Christians *et al.* 2015), this technology holds great promise to addressing our energy concerns. Addressing the issues of stability and use of lead can go a long way in maturing this technology for commercial application, though in the present legal framework use of lead is not a problem as CdTe based solar cell has received wide acceptance despite Cd content. Use of lead extensively in lead acid batteries and its content at comparable levels in CIGS and silicon modules to perovskites suggest that in the short term the concern may not be pressing, but these technologies are increasingly being phased out and alternatives are required to be explored to minimize the environmental impacts of these heavy metals. Replacement of lead with tin in perovskite solar cell is already under investigation and may also offer an environment friendly alternative (Noel *et al.* 2014).

The application of direct synthesized CNT network films as a hole collector for perovskite solar cells. The $CH_3NH_3PbI_3$/CNTs perovskite solar cell without hole-transporting material and Au electrode provided a power conversion efficiency of 6.29% under AM 1.5, 100 mW/cm$^2$ conditions and 8.85% under 10 mW/cm$^2$ conditions. The efficiency might be improved by future purification and chemical doping of CNTs to increase the film conductivity and increase the work function. Also, the utilization of pure semiconducting CNTs could increase the charge selectivity, improving the solar cell performance. By incorporating the hole transporting material spiro-OMeTAD, the $CH_3NH_3PbI_3$/CNTs perovskite solar cell efficiency can be further improved to 9.90%. (Li *et al*. 2014). With the advantages of low cost, a facile fabrication process without a vacuum environment, chemical stability and electrical compatibility to organometal halide perovskite, the CNT electrode is a promising electrode for replacement of expensive Au electrodes in perovskite solar cells. Furthermore, the flexible and transparent CNT film electrodes show great potential in flexible or tandem perovskite solar cells.

The next few years promise to be exciting ones for research and development of organic-inorganic halide perovskite solar cells. On-going efficiency improvements are expected, as well as a rapidly growing understanding of their material properties and optimal cell designs could be forthcoming. Advantages over existing photovoltaic technologies include material properties that simplify the manufacture of high-performance devices. The diversity in demonstrated approaches may give rise to low processing costs and simple implementation of attractive products, such as flexible, transparent or all perovskite tandem cell modules. This diversity may also allow perovskite cells to be directly integrated with other cell technologies to form high performance tandem cells; Si and CIGS modules appear particularly promising in this respect (Snaith, 2013; Service, 2014). In the present market, the toxicity of Pb is not a major impediment to large-scale, professional applications, as is evidenced by the fact that CdTe cells have already gained a reasonable market share. Cd or Pb is also present in some CIGS and silicon modules at the same general level as that likely in perovskite modules. The menace is that technology relying on toxic materials may be increasingly marginalized as legislation becomes increasingly more pervasive and restrictive.

## 9. CONCLUSION

The perovskite technology would allow the mass production of solar cells with high efficiency and at relatively low temperature, which would account for a substantial reduction of cost. Furthermore, flexible substrates could be used, which would allow an easier handling, transportation, installation and building integration of these new photovoltaic devices. Recently, transparent CNT networks had been proved to be good HTM as well as ETM and transparent electrode for perovskite solar cells. Film formation of the absorber layer is the key factor that determines the eventual performance of perovskite solar cells. The successful demonstration of high performance perovskite solar cells based on mesoporous oxide scaffolds has proven the importance of the film quality. This review paper also clearly demonstrated the influence of different type of HTMs and ETMs that were used to improve the performance and PCE of PrSCs. Further, higher efficiency is still possible through structural modification along with band gap tuning. Appropriate use of interfacial layers with high electrical conductivity between the electrodes and perovskite light absorber can increase the $V_{oc}$, $J_{sc}$ and FF of the device. Finally, substitution of other elements for Pb is one of the important tasks for environment friendly perovskite solar cells.

In order to bring about the success story of the R&D accomplishments and to convert the knowledge base to the technology and to the user finally, it is strongly suggested to reverse the prevailing trend where Indian Industry has little faith in indigenous R&D and has always fashioned licensing technical capabilities. In other words, there has been the gaps in the linkages between the scientists and the industrialists i.e., the research utility is to be considered inversely proportional to its distance from the industry and so the need of the hour is to revamp R&D institutions, Universities, etc. This is so because we have been trying to compete/collaborate with multinational R&D centers

who have been prompting us to accept their impositions. Indeed much could be said on these sides but little indeed is achievable if we don't focus on the corrective measures. Belief of the Indian industry to its internal R&D sector and support to further encourage innovations is mandatory for the self-reliance using "the Bowler's provisions compliant", Indian Patent act, no matter we can borrow anything that is worth from overseas manufacturers including from the USPTO and adopt & adapt them for the glory and prosperity of the nation in the area of our context, i.e., solar cells.

## REFERENCES


Abrusci, A., Stranks, S. D., Docampo, P., Yip, H. L., Jen, A. K. Y. and Snaith, H. J., High performance perovskite polymer hybrid solar cells via electronic coupling with fullerene monolayers, *Nano Lett.*, 13(7), 3124-3128(2013). doi:10.1021/nl401044q

Ball, J. M., Lee, M. M., Hey, A. and Snaith, H. J., Low-temperature processed meso superstructured to thin-film perovskite solar cells, *Energy Environ. Sci.*, 6(6), 1739(2013). doi:10.1039/c3ee40810h

Bi, D., Yang, L., Boschloo, G., Hagfeldt, A. and Johansson, E. M. J., Effect of different hole transport materials on recombination in $CH_3NH_3PbI_3$ perovskite-sensitized mesoscopic solar cells, *J. Phys. Chem. Lett.*, 4(9), 1532-1536(2013). doi:10.1021/jz400638x

Burghard, M., Electronic and vibrational properties of chemically modified single-wall carbon nanotubes, *Surf. Sci. Rep.*, 58(1-4), 1-109(2005). doi:10.1016/j.surfrep.2005.07.001

Burschka, J., Pellet, N., Moon, S. J., Humphry-Baker, R., Gao, P., Nazeeruddin, M. K. and Grätzel, M., Sequential deposition as a route to high-performance perovskite-sensitized solar cells, *Nat*., 499(7458), 316-320(2013). doi:10.1038/nature12340

Cai, B., Xing, Y., Yang, Z., Zhang, W. H. and Qiu, J., High performance hybrid solar cells sensitized by organolead halide perovskites, *Energy Environ. Sci.*, 6(5), 1480(2013). doi:10.1039/c3ee40343b

Cai, M., Tiong, V. T., Hreid, T., Bell, J. and Wang, H., An efficient hole transport material composite based on poly(3-hexylthiophene) and bamboo-structured carbon nanotubes for high performance perovskite solar cells, *J. Mater. Chem. A*, 3(6), 2784-2793(2015). doi:10.1039/c4ta04997g

Carnie, M. J., Charbonneau, C., Davies, M. L., Troughton, J. and Watson, T. M., Wojciechowski, K., Worsley, D. A., A one-step low temperature processing route for organolead halide perovskite solar cells, *Chem. Comm*., 49(72), 7893-7895(2013). doi:10.1039/c3cc44177f

Nam, C. Y., Wu, Q., Su, D., Chiu, C., Tremblay, N. J., Nuckolls, C. and Black, C. T., Nanostructured electrodes for organic bulk heterojunction solar cells: Model study using carbon nanotube dispersed polythiophene-fullerene blend devices, *J. Appl. Phys.*, 110(6), 64307(2011). doi.org/10.1063/1.3633236

Chen, Q., Zhou, H., Hong, Z., Luo, S., Duan, H. S., Wang, H. H. and Yang, Y., Planar Heterojunction perovskite solar cells via vapor-assisted solution process, *J. Am. Chem. Soc.*, 136(2), 622-625(2014). doi:10.1021/ja411509g

Chiang, C. H., Tseng, Z. L. and Wu, C. G., Planar heterojunction perovskite/$PC_{71}BM$ solar cells with enhanced open circuit voltage via a (2/1)-step spin-coating process, *J. Mater. Chem. A*, 2, 15897-15903(2014). doi: 10.1039/c4ta03674c

Christians, J. A., Fung, R. C. M. and Kamat, P. V., An inorganic hole conductor for organo lead halide perovskite solar cells- Improved hole conductivity with copper iodide, *J. Am. Chem. Soc.*, 136(2), 758-764(2014). doi:10.1021/ja411014k

Christians, J. A., Manser, J. S. and Kamat, P. V., Best practices in perovskite solar cell efficiency measurements- avoiding the error of making bad cells look good, *J. Phys. Chem. Lett.*, 6(5), 1-13(2015). doi:10.1021/acs.jpclett.5b00289

Chung, I., Lee, B., He, J., Chang, R. P. and Kanatzidis, M. G., All solid-state dye-sensitized solar cells with high efficiency, *Nat.*, 485(7399), 486-489(2012). doi:10.1038/nature11067

De Jong, M. P., Van IJzendoorn, L. J. and De Voigt, M. J. A., Stability of the interface between indium-tin-oxide and poly(3,4-ethylenedioxythiophene)/poly(styrenesulfonate) in polymer light-emitting diodes, *Appl. Phys. Lett*., 77(14), 2255-2257(2000). doi:10.1063/1.1315344

Dobrzańska-Danikiewicz, A. D. and Drygała, A., Strategic development perspectives of laser processing on polycrystalline silicon surface, *Arch. Mater. Sci. Eng*., 50(1), 5-20(2011).

Dobrzański, L.A., Drygała, A. and Prokopiuk vel Prokopowicz, M., Selection of components for photovoltaic system, *Arch. Mater. Sci. Eng.*, 62(2), 53-59(2013).

Docampo, P., Ball, J. M., Darwich, M., Eperon, G. E and Snaith, H. J., Efficient organo etal trihalide perovskite planar-heterojunction solar cells on flexible polymer substrates, *Nat. Comm.*, 4, 2761(2013). doi:10.1038/ncomms3761

Bi, D., Yang, L., Boschloo, G., Hagfeldt, A., and Erik M. J. Johansson, Effect of different hole transport materials on recombination in $CH_3NH_3PbI_3$ perovskite-sensitized mesoscopic solar cells, *J. Phys. Chem. Lett.*, 4(9), 1532-1536(2013). doi: 10.1021/jz400638x

Edri, E., Kirmayer, S., Cahen, D. and Hodes, G., High Open-Circuit Voltage Solar Cells Based on Organic/Inorganic Lead Bromide Perovskite, *J. Phys. Chem. Lett.*, 4(6), 897-902(2013). doi: 10.1021/Jz400348

Eperon, G. E., Stranks, S. D., Menelaou, C., Johnston M. B. and Herz, L. M., Formamidinium lead trihalide: a broadly tunable perovskite for efficient planar heterojunction solar cells, *Energy Environ. Sci.* 7(3), 982-988(2014). doi: 10.1039/C3EE43822H

Frank, S., Poncharal, P., Wang, Z.L. and de Heer, W.A., Carbon nanotube quantum resistors, *Sci*., 280(537), 1744-1746(1998). doi: 10.1126/science.280.5370.1744

Gillet, M., Aguir, K., Lemire, C., Gillet, E. and Schierbaum, K., The structure and electrical conductivity of vacuum-annealed $WO_3$ thin films, *Thin Solid Films*, 467(1-2), 239-246(2004). doi:10.1016/j.tsf.2004.04.018

Gratzel, C. and Zakeeruddin, S.M., Recent trends in mesoscopic solar cells based on molecular and nanopigment light harvesters, *Mater. Today*, 16(1-2), 11-18(2013). doi:10.1016/j.mattod.2013.01.020

Han, T. H., Lee, Y., Choi, M. R., Woo, S. H., Bae, S. H., Hong, B. H., Ahn, J. H. and Lee, T. W., Extremely efficient flexible organic light-emitting diodes with modified graphene anode, *Nat. Photonics*, 6(2),105-110(2012). doi:10.1038/nphoton.2011.318

Hardin, B. E., Snaith, H. J. and McGehee, M. D., The renaissance of dye sensitized solar cells, *Nat. Photonics*, 6(3), 162-169(2012). doi:10.1038/nphoton.2012.22

Im, J. H., Lee, C. R., Lee, J. W., Park, S. W. and Park, N. G., 6.5% Efficient Perovskite Quantum-Dot-Sensitized Solar Cell, *Nanoscale*, 3(10), 4088(2011). doi:10.1039/c1nr10867k

Jeon, N. J., Lee, J., Noh, J.H., Nazeeruddin, M. K., Grätzel, M. and Seok, S. I., Efficient inorganic-organic hybrid perovskite solar cells based on pyrene arylamine derivatives as hole-transporting materials, *J. Amer. Chem. Soc*., 135(51), 19087-19090(2013). doi:10.1021/ja410659k

Kalaiselvan, S., Balachandran, K., Karthikeyan, S. and Venckatesh, R., Botanical Hydrocarbon sources based by spray pyrolysis method for DSSC applications, *Silicon*, 8(3), 1-7(2016). doi:10.1007/s12633-016-9419-7

Kamat, P. V., Quantum Dot Solar Cells, The Next Big Thing in Photovoltaics, *J. Phys. Chem. Lett*., 4(6), 908-918(2013). doi:10.1021/jz400052e

Kim, B. J., Kim, dong, H., Lee, Y. Y., Shin, H. W., Han, G. S., Hong, J. S. and Jung, H. S., Highly efficient and bending durable perovskite solar cells toward wearable power source, *Energy Environ. Sci.*, 8(3), 916-921(2015). doi:10.1039/c4ee02441a

Kim, H., Lim, K. G. and Lee, T. W., Planar heterojunction organometal halide perovskite solar cells: roles of interfacial layers, *Energy Environ. Sci.*, 9(1), 12-30(2016). doi:10.1039/C5EE02194D

Kim, H., Bae, S. H., Han, T. H., Lim, K. G., Ahn, J. H. and Lee, T. W., Organic solar cells using CVD grown graphene electrodes, *Nanotech.*, 25(1), 014012(2014). doi:10.1088/0957-4484/25/1/014012

Kim, H. S., Lee, C. R., Im, J. H., Lee, K. B., Moehl, T., Marchioro, A. and Park, N. G., Lead iodide perovskite sensitized all-solid-state submicron thin film mesoscopic solar cell with efficiency exceeding 9%, *Sci. Rep.*, 2(7436), 591( 2012). doi:110.1038/srep00591

Kim, H. S., Mora-Sero, I., Gonzalez-Pedro, V., Fabregat-Santiago, F., Juarez-Perez, E. J., Park, N. G. and Bisquert, J., Mechanism of carrier accumulation in perovskite thin-absorber solar cells, *Nat. Comm.*, 4, 2242(2013). doi:10.1038/ncomms3242

Kojima, A., Teshima, K., Shirai, Y. and Miyasaka, T., Organometal halide perovskites as visible-light sensitizers for photovoltaic cells, *J. Am. Chem. Soc*., 131(17), 6050-6051(2009). doi:10.1021/ja809598r

Kojima, A., Teshima, K., Shirai, Y. and Miyasaka, T., Novel photoelectrochemical cell with mesoscopic electrodes sensitized by lead-halide compounds, *ECS Meeting*, 27, MA2008-02(2008).

Lee, M. M., Teuscher, J., Miyasaka, T., Murakami, T. N. and Snaith, H. J., Efficient hybrid solar cells based on meso-superstructured organometal halide perovskites, *Sci.*, 338(6107), 643-647(2012). doi:10.1126/science.1228604

Lee, S. J., Kim, Y. H., Kim, J. K., Baik, H., Park, J. H., Lee, J., Nam, J., Park, J. H., Lee, T. W., Yi, G. R. and Cho, J. H., A roll-to-roll welding process for planarized silver nanowire electrodes, *Nanoscale*, 6(20), 11828-11834(2014). doi: 10.1039/C4NR03771E

Li, Z., Kulkarni, S.A., Boix, P.P., Shi, E., Cao, A., Fu, K., Mhaisalkar, S.G., Laminated carbon nanotube networks for metal electrode-free efficient perovskite solar cells, *ACS Nano*, 8(7), 6797-6804(2014). doi:10.1021/nn501096h

Li, C., Wang, F., Xu, J., Yao, J., Zhang, B., Zhang, C., Xiao, M., Dai, S., Li, Y. and Tan, Z., Efficient perovskite/fullerene planar heterojunction solar cells with enhanced charge extraction and suppressed charge recombination, Nanoscale, 7(21), 9771-9778(2015). doi: 10.1039/c4nr06240j

Liang, P. W., Chueh, C. C., Xin, X. K., Zuo, F., Williams, S. T., Liao, C. Y. and Jen, A. K. Y., High-performance planar-heterojunction solar cells based on ternary halide large-band-gap perovskites, *Adv. Energy Mater*., 5(1), (2015). doi:10.1002/aenm.201400960

Liang, P. W., Liao, C. Y., Chueh, C. C., Zuo, F., Williams, S. T., Xin, X. K., Jen, A. K. Y., Additive enhanced crystallization of solution processed perovskite for highly efficient planar heterojunction solar cells, *Adv. Mater*., 26(22), 3748-3754(2014). doi:10.1002/adma.201400231

Lin, Q., Armin, A., Nagiri, R. C. R., Burn, P. L. and Meredith, P., Electro-optics of perovskite solar cells, *Nat. Photonics*, 9(2), 106-112(2015). doi:10.1038/nphoton.2014.284

Liu, D., Gangishetty, M. K. and Kelly, T. L., Effect of $CH_3NH_3PbI_3$ thickness on device efficiency in planar heterojunction perovskite solar cells, *J. Mater. Chem.* A, 2(46), 19873-19881(2014). doi:10.1039/C4TA02637C

Liu, D. and Kelly, T. L., Perovskite solar cells with a planar heterojunction structure prepared using room-temperature solution processing techniques, *Nat. Photonics*, 8(2), 133-138(2013). doi:10.1038/nphoton.2013.342

Liu, M., Johnston, M. B. and Snaith, H. J., Efficient planar heterojunction perovskite solar cells by vapour deposition, *Nat*., 501(7467), 395-398(2013). doi:10.1038/nature12509

Liu, C., Wang, K., Du, P., Meng, T., Yu, X., Cheng, S.Z.D. and Gong, X., High performance planar heterojunction perovskite solar cells with fullerene derivatives as the electron transport layer, *ACS Appl. Mater. Interfaces*, 7(2), 1153-1159(2015). doi: 10.1021/am506869k

Liu, X., Jiao, W., Lei, M., Zhou, Y., Song, B. and Li, Y., Crown-ether functionalized fullerene as a solution-processable cathode buffer layer for high performance perovskite and polymer solar cells, *J. Mater. Chem*. A, 3(17), 9278-9284(2015). doi: 10.1039/c4ta05881j

Lu, L., Joannopoulos, J. D. and Soljacic, M., Topological photonics, *Nat. Photon*, 8(11), 821-829 (2014). doi:10.1038/nphoton.2014.248

Malinkiewicz, O., Yella, A., Lee, Y. H., Espallargas, G. M. M., Graetzel, M., Nazeeruddin, M. K. and Bolink, H. J., Perovskite solar cells employing organic charge transport layers, *Nat. Photonics*, 8(2), 128-132(2014). doi:10.1038/nphoton.2013.341

Min, J., Zhang, Z. G., Hou, Y., Quiroz, C. O. R., Przybilla, T., Bronnbauer, C., … and Brabec, C. J., Interface engineering of perovskite hybrid solar cells with solution-processed perylene-diimide heterojunctions toward high performance, *Chem. Mater*., 27(1), 227-234(2015). doi.org/10.1021/cm5037919

Nam, C. Y., Wu, Q., Su, D., Chiu, C., Tremblay, N. J., Nuckolls, C. and Black, C. T., Nanostructured electrodes for organic bulk heterojunction solar cells: Model study using carbon nanotube dispersed polythiophene-fullerene blend devices, *J. Appl. Phys*., 110(6), 64307(2011). doi:10.1063/1.3633236

Nayak, P. K., Perovskite solar cells: an emerging photovoltaic technology, *Adv. Mater*., 18(2), 65-72(2014). doi:10.1002/ adma.201304620

Noel, N. K., Stranks, S. D., Abate, A., Wehrenfennig, C., Guarnera, S., Haghighirad, A. A.,Snaith, H. J., Lead-free organic-inorganic tin halide perovskites for photovoltaic applications, *Energy Environ. Sci*., 7(9), 3061-3068(2014). doi:10.1039/c4ee01076k

Noh, J. H., Im, S. H., Heo, J. H., Mandal, T. N. and Seok, S. I., Chemical management for colorful, efficient and stable inorganic-organic hybrid nanostructured solar cells, *Nano Lett.*, 13(4), 1764-1769(2013). doi:10.1021/nl400349b

Ogomi, Y., Morita, A., Tsukamoto, S., Saitho, T., Fujikawa, N., Shen, Q., Hayase, S., $CH_3NH_3Sn_xPb_{(1-x)}I_3$ perovskite solar cells covering up to 1060 nm, *J. Phys. Chem. Lett*., 5(6), 1004-1011(2014). doi:10.1021/jz5002117

O'Regan, B., Gratzel, M., A low-cost, high-efficiency solar cell based on dye-sensitized colloidal $TiO_2$ films, *Nat*., 353, 737-740(1991). doi:10.1038/353737a0

Paek, S., Cho, N., Choi, H., Jeong, H., Lim, J.S., Hwang, J. Y., Lee, J. K. and Ko, J., Improved external quantum efficiency from solution processed $CH_3NH_3PBI_3$ perovskite/PC71BM planer heterojunction for high efficiency hybrid solar cells, *J. Phys. Chem. C*, 118(45), 25899-25905(2014). doi: 10.1021/jp508162p

Park, N. G., Organometal perovskite light absorbers toward a 20% efficiency low-cost solid-state mesoscopic solar cell, *J. Phys. Chem. Lett*., 4(15), 2423-2429(2013). doi:10.1021/jz400892a

Park, N. G., Perovskite solar cells: An emerging photovoltaic technology, *Mater. Today*, 18(2), 65-72(2015). doi:10.1016/j.mattod.2014.07.007

Qin, P., Domanski, A. L., Chandiran, A. K., Berger, R., Butt, H. J., Dar, M. I., … and Grätzel, M., Yttrium-substituted nanocrystalline $TiO_2$ photoanodes for perovskite based heterojunction solar cells, *Nanoscale*, 6(3), 1508-1514(2014). doi.org/10.1039/c3nr05884k

Poorkazem, K., Liu, D. and Kelly, T. L., Fatigue resistance of a flexible, efficient and metal oxide-free perovskite solar cell, *J. Mater. Chem. A*, 3(17), 9241-9248(2015). doi:10.1039/c5ta00084j

Qiu, J., Qiu, Y., Yan, K., Zhong, M., Mu, C., Yan, H. and Yang, S., All-solid-state hybrid solar cells based on a new organometal halide perovskite sensitizer and one-dimensional $TiO_2$ nanowire arrays, *Nanoscale*, 5(8), 3245-3248(2013). doi:10.1039/c3nr00218g

Roldan-Carmona, C., Malinkiewicz, O., Soriano, A., Minguez Espallargas, G., Garcia, A., Reinecke, P., Bolink, H. J., Flexible high efficiency perovskite solar cells, *Energy Environ. Sci*., 7(3), 994-997(2014). doi:10.1039/c3ee43619e

Schulz, P., Whittaker-Brooks, L. L., MacLeod, B. A., Olson, D. C, Loo, Y. L. and Kahn, A., Electronic level alignment in inverted organometal perovskite solar cells, *Adv. Mater. Interface.*, 2(7), 1400532(2015). doi: 10.1002/admi.201400532

Service, R. F., Turning up the light, *Sci.*, 342(6160), 794-795,797(2013). doi:10.1126/science.342.6160.794

Service, R. F., Perovskite Solar Cells Keep On Surging, Science, 344(6183), 458(2014). doi:10.1126/science.344.6183.458

Shao, Y., Xiao, Z., Bi, C., Yuan, Y. and Huang, J., Origin and elimination of photocurrent hysteresis by fullerene passivation in $CH_3NH_3PbI_3$ planar heterojunction solar cells, *Nat. Comm.*, 5, 5784(2014). doi: 10.1038/ncomms6784

Shi, Y., Wang, K., Du, Y., Zhang, H., Gu, J., Zhu, C. and Ma, T., Solid-state synthesis of ZnO nanostructures for quasi-solid dye-sensitized solar cells with high efficiencies up to 6.46%, *Adv. Mater*., 25(32), 4413-4419(2013). doi:10.1002/adma.201301852

Shiraishi, M. and Ata, M., Work function of carbon nanotubes, *Carbon*, 39(12), 1913-1917(2001). doi:10.1016/S0008-6223(00)00322-5

Snaith, H. J., Estimating the maximum attainable efficiency in dye-sensitized solar cells, *Adv. Funct. Mater*., 20(1), 13-19(2010). doi:10.1002/adfm.200901476

Snaith, H. J., Perovskites: The emergence of a new era for low-cost, high performance perovskite solar cells, *J. Phys. Chem. Lett.*, 4(21), 3623-3630(2013). doi:10.1021/jz4020162

Snaith, H. J. and Grätzel, M., Enhanced charge mobility in a molecular hole transporter via addition of redox inactive ionic dopant: Implication to dye-sensitized solar cells, *Appl. Phys. Lett.*, 89(26), 262114(2006). doi:10.1063/1.2424552

Snaith, H. J. and Grätzel, M., Electron and hole transport through mesoporous $TiO_2$ infiltrated with spiro-MeOTAD, *Adv. Mater*., 19(21), 3643-3647(2007). doi:10.1002/adma.200602085

Solar, P., Li, Z., Kulkarni, S. A., Boix, P. P., Shi, E., Cao, A., atabyal, S. K., Laminated Carbon Nanotube Networks for Metal Electrode-Free, *ACS Nano*, 8(7), 6797-6804(2014). doi:10.1021/nn501096h

Song, T. B., Chen, Q., Zhou, H., Jiang, C., Wang, H. H., and Yang, Y., Perovskite solar cells: film formation and properties, *J. Mater. Chem. A*, 3(17), 9032-9050(2015). doi:10.1039/c4ta05246c

Song, X., Wang, W., Sun, P., Ma, W. and Chen, Z. K., Additive to regulate the perovskite crystal film growth in planar heterojunction solar cells, *Appl. Phys. Lett*., 106(3), 033901(2015). doi:10.1063/1.4906073

Stoumpos, C. C., Malliakas, C. D. and Kanatzidis, M. G., Semiconducting tin and lead iodide perovskites with organic cations: Phase transitions, high mobilities, and near-infrared photoluminescent properties, *Inorg. Chem.*, 52(15), 9019-9038(2013). doi:10.1021/ic401215x

Stranks, S. D., Eperon, G. E., Grancini, G., Menelaou, C., Alcocer, M. J. P., Leijtens, T., Miura, N., Electron-hole diffusion lengths exceeding 1 micrometer in an organometal trihalide perovskite absorber, *Sci.*, 342(6156), 341-344(2013). doi:10.1126/science.1243982

Ulbricht, R., Lee, S. B., Jiang, X., Inoue, K., Zhang, M., Fang, S., Zakhidov, A. A., Transparent carbon nanotube sheets as 3-D charge collectors in organic solar cells, *Sol. Energy Mater. Sol. Cells*., 91(5), 416-419(2007). doi:10.1016/j.solmat.2006.10.002

Yin, W. J., Shi, T. and Yan, Y., Unique properties of halide perovskites as possible origins of the superior solar cell performance, *Adv. Mater.*, 26(27), 4653-4658(2014). doi.org/10.1002/adma.201306281

Wang, X., Li, Z., Xu, W., Kulkarni, S. A., Batabyal, S. K., Zhang, S., Wong, L. H., $TiO_2$ nanotube arrays based flexible perovskite solar cells with transparent carbon nanotubes electrode, *Nano Energy*, 11, 728-735(2015). doi:10.1016/j.nanoen.2014.11.042

Wang, J., Ball, J., Barea, E., Alexander-Webber, A., Huang, J., Saliba, M., Mora-Sero, I., Bisquert, J. and Snaith, H., Low-Temperature Processed Electron Collection Layers of Graphene/$TiO_2$ Nanocomposites in Thin Film Perovskite Solar Cells, *Nano Lett.*, 14(2), 724−730(2014). doi: 10.1021/nl403997a

Wang, F., Valentin, C. and Pacchioni, G., Rational band gap engineering of $wo_3$ photocatalyst for visible light water splitting, *Chem. Cat. Chem.*, 4(4), 476−478(2012). doi: 10.1002/cctc.201100446

Wang, Q. K., Wang, R. B., Shen, P. F., Li, C., Li, Y. Q., Liu, L. J., Duhm, S. and Tang, J. X., Energy level offsets at lead halide perovskite/organic hybrid interfaces and their impacts on charge separation, *Adv. Mater. Interfaces*, 2(3), 1400528(2015). doi: 10.1002/admi.201400528

Wang, K., Shi, Y., Dong, Q., Li, Y., Wang, S., Yu, X., Wu, M. and Ma, T., Low-temperature and solution-processed amorphous WO X as electron-selective layer for perovskite solar cells, *J. Phys. Chem. Lett.*, 6(5), 755-759(2015). doi: 10.1021/acs.jpclett.5b00010

Wang, K. C., Jeng, J. Y., Shen, P. S., Chang, Y. C., Diau, E. W. G., Tsai, C. H., Chao, T. Y., Hsu, H. C., Lin, P. Y., Chen, P., Guo, T. F. and Wen, T. C., p-type mesoscopic nickel oxide/organometallic perovskite heterojunction solar cells, *Sci. Rep.*, 4, 4756(2014). doi: 10.1038/srep04756

Wojciechowski, K., Saliba, M., Leijtens, T., Abate, A. and Snaith, H. J., Sub-150 °C processed meso-superstructured perovskite solar cells with enhanced efficiency, *Energy Environ. Sci.*, 7(3), 1142-1147(2014). doi:10.1039/c3ee43707h

Wu, Z., Bai, S., Xiang, J., Yuan, Z., Yang, Y., Cui, W., Sun, B., Efficient planar heterojunction perovskite solar cells employing graphene oxide as hole conductor, *Nanoscale*, 6(18), 10505-10510(2014). doi:10.1039/c4nr03181d

Xiao, Z., Bi, C., Shao, Y., Dong, Q., Wang, Q., Yuan, Y., Wang, C., Gao, Y. and Huang, J., efficient, high yield perovskite photovoltaic devices grown by interdiffusion of solution-processed precursor stacking layers, *Energy Environ. Sci.*, 7(8), 2619-2623(2014). doi: 10.1039/c0ee00278j

Yella, A., Heiniger, L. P., Gao, P., Nazeeruddin, M. K. and Gratzel, M., Nanocrystalline rutile electron extraction layer enables low-temperature solution processed perovskite photovoltaics with 13.7% efficiency, *Nano Lett.*, 14(5), 2591-2596(2014). doi:10.1021/nl500399m

Yeo, J. S., Kang, R., Lee, S., Jeon, Y. J., Myoung, N., Lee, C. L., Kim, D. Y., Yun, J. M., Seo, Y. H., Kim, S. S. and Na, S. I., Highly efficient and stable planar perovskite solar cells with reduced graphene oxide nanosheets as electrode interlayer, *Nano Energy*, 12, 96-104(2015). doi:10.1016/j.nanoen.2014.12.022

Yin, W. J., Shi, T. and Yan, Y., Unique properties of halide perovskites as possible origins of the superior solar cell performance, *Adv. Mater.*, 26(27), 4653-4658(2014). doi:/10.1002/adma.201306281

You, J., Hong, Z., Yang, Y. M., Chen, Q., Cai, M., Song, T., Ang, Y., Low-temperature solution-processed perovskite solar cells with high efficiency and flexibility, *ACS Nano*, 8(2), 1674-1680(2014). doi:10.1021/nn406020d

You, J., Yang, Y., Hong, Z., Song, T. B., Meng, L., Liu, Y., Jiang, C., Zhou, H., Chang, W. H., Li, G. and Yang, Y., Moisture assisted perovskite film growth for high performance solar cells, *Appl. Phys. Lett.*, 105(18), 183902(2014). doi:10.1063/1.4901510

Yu, K. and Chen, J., Enhancing solar cell efficiencies through 1-D nanostructures, *Nanoscale Res. Lett.*, 4(1), 1-10(2009). doi:10.1007/s11671-008-9200-y

Zhang, Q. F., Dandeneau, C. S., Zhou, X. Y. and Cao, G. Z., ZnO nanostructures for dye sensitized solar cells, *Adv. Mater.*, 21(41), 4087-4108(2009). doi:10.1002/adma.200803827

Zhang, H., Azimi, H., Hou, Y., Ameri, T., Przybilla, T., Spiecker, E., Kraft, M., Scherf, U. and Brabec, C. J., Improved high-efficiency perovskite planar heterojunction solar cells via incorporation of a polyelectrolyte interlayer, *Chem.Mater.*, 26, 5190-5193(2014). doi: 10.1021/cm502864s

Zhao, D., Sexton, M., Park, H. Y., Baure, G., Nino, J. C. and So, F., High-efficiency solution-processed planar perovskite solar cells with a polymer hole transport layer, *Adv. Energy Mater.*, 5(6), 1401855(2015). doi: 10.1002/aenm.201401855

Wu, Z., Bai, S., Xiang, J., Yuan, Z., Yang, Y., Cui, W. and Sun, B., Efficient planar heterojunction perovskite solar cells employing graphene oxide as hole conductor, *Nanoscale*, 6(18), 10505-10510(2014). doi.org/10.1039/C4NR03181D

Zhou, H. P., Chen, Q., Li, G., Luo, S., Song, T. B., Duan, H. S.,Yang, Y., Interface engineering of highly efficient perovskite solar cells, *Sci.*, 345(6196), 542-546(2014). doi:10.1126/science.1254050

Zhou, Y., Fuentes-Hernandez, C., Shim, J., Meyer, J., Giordano, A. J., Li, H., Winget, P., Papadopoulos, T., Cheun, H., Kim, J., Fenoll, M., Dindar, A., Haske, W., Najafabadi, E., Khan, T. M., Sojoudi, H., Barlow, S., Graham, S., Brédas, J. L., Marder, S. R., Kahn, A. and Kippelen, B., A universal method to produce low-work function electrodes for organic electronics, *Sci.*, 336(6079), 327-332(2012). doi: 10.1126/science.1218829